The MAL Proteolipid Is Necessary for Normal Apical Transport and Accurate Sorting of the Influenza Virus Hemagglutinin in Madin-Darby Canine Kidney Cells

Rosa Puertollano,* Fernando Martín-Belmonte,* Jaime Millán,* María del Carmen de Marco,* Juan P. Albar,‡ Leonor Kremer,‡ and Miguel A. Alonso*

*Centro de Biología Molecular "Severo Ochoa," Universidad Autónoma de Madrid and Consejo Superior de Investigaciones Científicas, and ‡Department of Immunology and Oncology, Centro Nacional de Biotecnología, Consejo Superior de Investigaciones Científicas, Cantoblanco, 28049-Madrid, Spain

Abstract. The MAL (MAL/VIP17) proteolipid is a nonglycosylated integral membrane protein expressed in a restricted pattern of cell types, including T lymphocytes, myelin-forming cells, and polarized epithelial cells. Transport of the influenza virus hemagglutinin (HA) to the apical surface of epithelial Madin-Darby canine kidney (MDCK) cells appears to be mediated by a pathway involving glycolipid- and cholesterol-enriched membranes (GEMs). In MDCK cells, MAL has been proposed previously as being an element of the protein machinery for the GEM-dependent apical transport pathway. Using an antisense oligonucleotide-based strategy and a newly generated monoclonal antibody to canine MAL, herein we have approached the effect of MAL depletion on HA transport in MDCK cells. We have found that MAL depletion diminishes the presence of HA in GEMs, reduces the rate of HA transport to the cell surface, inhibits the delivery of HA to the apical surface, and produces partial missorting of HA to the basolateral membrane. These effects were corrected by ectopic expression of MAL in MDCK cells whose endogenous MAL protein was depleted. Our results indicate that MAL is necessary for both normal apical transport and accurate sorting of HA.

Key words: apical transport • glycolipid-enriched membranes • sorting • Madin-Darby canine kidney cells • proteolipids

THE elucidation of the molecular mechanisms involved in the generation and maintenance of an asymmetric distribution of cell-surface components is a major concern of contemporary cell biology (Matter and Mellman, 1994; Eaton and Simons, 1995; Drubin and Nelson, 1996). This asymmetry is quite evident in the case of polarized epithelial cells in which the plasma membrane is subdivided into two morphologically, functionally, and biochemically different surfaces: the apical domain, that faces the organ lumen, and the basolateral domain, which contacts adjacent cells and the basement membrane. Most studies on polarized transport have been carried out using the Madin-Darby canine kidney (MDCK)[1] cell line, which is considered to be an archetype of polarized epithelial cells (Rodriguez-Boulan and Powell, 1992). The seminal observation that some enveloped RNA viruses bud asymmetrically from MDCK cells led to the generalized use of viruses for deciphering the mechanisms of sorting to the apical or the basolateral surfaces (Rodriguez-Boulan and Sabatini, 1978; Roth et al., 1979). The influenza virus buds apically in MDCK cells, and the viral envelope hemagglutinin (HA) glycoprotein is transported specifically to the apical surface (Rodriguez-Boulan and Pendergast, 1980). Over the last two decades, transport of influenza virus HA in MDCK cells has been considered to be a paradigm for the study of the mechanism for apical sorting of integral membrane proteins in epithelial cells (Rodriguez-Boulan and Powell, 1992; Matter and Mellman, 1994).

Segregation of newly synthesized proteins in distinct transport vesicles destined for either the apical or basolateral surface takes place in the trans-Golgi network (Keller and Simons, 1997; Traub and Kornfeld, 1997). Basolateral delivery of transmembrane proteins is mediated by sequences present in their cytoplasmic tail that may or may not be related to tyrosine- or di-leucine–based sorting sig-

Address correspondence to Miguel A. Alonso, Centro de Biología Molecular "Severo Ochoa," Universidad Autónoma de Madrid, Cantoblanco, 28049-Madrid, Spain. Tel.: 34-91-397-8037. Fax: 34-91-397-8087. E-mail: maalonso@ cbm.uam.es

1. *Abbreviations used in this paper:* d, dog; GEM, glycolipid- and cholesterol-enriched membrane; h, human; HA, hemagglutinin; MDCK, Madin-Darby canine kidney; sulfo-NHS-biotin, sulfo-*N*-hydroxyl-succinimido-biotin.

nals. However, the identification of peptide signals for apical sorting of integral membrane remained elusive (Keller and Simons, 1997). Although glycation appears to be necessary for apical transport of certain transmembrane glycoproteins (Gut et al., 1998), obviously it is not required for nonglycosylated apical proteins (Alonso et al., 1997). Moreover, influenza virus HA requires neither glycans nor its cytoplasmic tail for apical sorting (Green et al., 1981; Thomas and Roth, 1994). Glycolipids are highly enriched in the apical membrane (Simons and van Meer, 1988). Glycolipids and cholesterol form tight clusters that are resistant to solubilization by nonionic (e.g., Triton X-100) detergents (Hanada et al., 1995). The fact that HA becomes insoluble in Triton X-100 after biosynthesis (Skibbens et al., 1989) led to the suggestion that HA, and probably other membrane proteins, are cosorted with glycolipids in vesicular carriers destined for the apical membrane (Simons and Wandinger-Ness, 1990). According to this model, the compatibility of certain proteins with these glycolipid- and cholesterol-enriched membrane (GEM) clusters or "rafts" constitutes the basis for their selective sorting to the apical domain. It was proposed that GEMs require protein sorting machinery to be operative as a route of transport. The minimal components of this machinery would consist of a set of proteins to carry out the processes of vesicle formation, cargo recruiting, targeting, and fusion to the apical surface (Simons and Wandinger-Ness, 1990).

The *MAL* gene was identified 12 years ago during a search for genes differentially expressed during human T cell development (Alonso and Weissman, 1987). More recently, the MAL protein has been identified in rat myelin-forming cells (Kim et al., 1995; Schaeren-Wiemers et al., 1995), and in polarized epithelial cells, including the renal MDCK cell line (MAL/VIP17) (Zacchetti et al., 1995; Millán et al., 1997a) and thyroid cells (Martín-Belmonte et al., 1998). The *MAL* gene encodes a nonglycosylated integral membrane protein of 17 kD containing multiple hydrophobic segments (Alonso and Weissman, 1987). In contrast with most integral membrane proteins, MAL displays unusual lipid-like properties that make it highly soluble in organic solvents used to extract cell lipids (Martín-Belmonte et al., 1998). In addition, MAL shares with a restricted group of integral membrane proteins the distinctive biochemical feature of residence in GEMs in all of the cell types in which it is expressed (Kim et al., 1995; Zacchetti et al., 1995; Martín-Belmonte et al., 1998; Millán and Alonso, 1998). MAL is localized to the apical zone of thyroid epithelial cells in intact follicles (Martín-Belmonte et al., 1998), and it has been identified in an MDCK cellular fraction containing transport vesicles enriched with apically destined proteins (Zacchetti et al., 1995). Together, these observations fulfill the requirements predicted for the hypothetical components of the integral membrane protein machinery for GEM-dependent transport. Furthermore, the observation that ectopic expression of MAL in insect Sf21 cells produces a massive de novo formation of vesicles led to the proposal of MAL as a putative component of the machinery responsible for GEM vesiculation (Puertollano et al., 1997). However, the definitive confirmation of candidate proteins as components of the apical sorting machinery depends on direct evidence of their requirement for transport of cargo proteins.

We have directly investigated the possible role of MAL in apical transport by studying the polarized delivery of HA in the prototypical system of MDCK cells infected with influenza virus. Using a newly generated mAb specific to dog MAL (dMAL), we have been able to quantify the extent of the depletion obtained in the endogenous protein upon transfection of an antisense oligonucleotide complementary to dMAL mRNA. Using this strategy we have found that MAL depletion diminishes the presence of HA in GEMs, reduces the rate of HA transport to the cell surface, inhibits the delivery of HA to the apical surface, and produces partial missorting of HA to the basolateral membrane. These effects were corrected by ectopic expression of human MAL (hMAL) in MDCK cells with the endogenous protein depleted. These results indicate that MAL is necessary for accurate transport of HA to the apical surface, and highlights the role of MAL as a component of the integral protein machinery for GEM-mediated apical transport.

Materials and Methods

Materials

The mouse hybridomas producing mAb 9E10 against the c-Myc epitope EQKLISEED (Evan et al., 1985) or mAb OKT4 to the human CD4 molecule were obtained from the American Type Culture Collection. Mouse mAbs to E-cadherin, calnexin, or caveolin were obtained from Transduction Labs. The anti-amyloid precursor protein antibody was from Boehringer Mannheim. Peroxidase-conjugated secondary anti-Ig antibodies, sulfo-*N*-hydroxyl-succinimido-biotin (sulfo-NHS-biotin), streptavidin-coupled agarose, and peroxidase-coupled streptavidin were supplied by Pierce. Triton X-100 and octyl-glucoside were purchased from Sigma Chemical Co.

Cell Culture and Infection Conditions

Epithelial MDCK II cells from canine kidney were grown on Petri dishes in DME supplemented with 10% of FBS (GIBCO BRL), penicillin (50 U/ml), and streptomycin (50 μg/ml) at 37°C in an atmosphere of 5% CO_2. Influenza virus A/Victoria/3/75 (H3N2) strain (a generous gift from Dr. J. Ortín, Centro Nacional de Biotecnología, Madrid) was grown and titered on MDCK cells. Confluent cell monolayers were incubated with influenza virus (10 pfu/cell) for 1 h at 37°C to allow adsorption and entry of the virus. After that (taken as time 0 of infection), the inoculum was removed and the cell cultures were incubated at 37°C for the indicated times in normal medium.

Preparation of mAbs to dMAL

The decapeptide QEGYTYKQYH corresponding to amino acids 114–123 of the dMAL molecule was synthesized on an automated multiple peptide synthesizer (AMS 422; Abimed) using the solid phase procedure and standard Fmoc-chemistry (Gausepohl et al., 1992). After coupling to keyhole limpet hemocyanin, the peptide was used to immunize Wistar rats. Spleen cells from immunized rats were fused to myeloma cells following standard protocols (Harlow and Lane, 1988), and plated onto microtiter plates. The culture supernatants were screened by immunoblot analysis using GEMs from MDCK cells. The hybridoma clone 2E5 that secretes antibodies to dMAL was isolated after several rounds of screening, and used to produce culture supernatants containing 2E5 mAb.

DNA Constructions, Oligonucleotides, and Transfections

The DNA constructs expressing the hMAL or dMAL proteins tagged at their NH_2 terminus with the 9E10 c-Myc epitope, and the A498 and MDCK stable transfectants expressing tagged hMAL (A498/hMAL and MDCK/hMAL cells) have been described previously (Millán et al., 1997a,b; Martín-Belmonte et al., 1998). Transient transfection of COS-7

cells with constructs expressing either hMAL or dMAL was carried out by electroporation using Electro Cell Manipulator 600 equipment (BTX). Phosphorothioate oligonucleotides were synthesized with sulfur throughout the phosphate backbone (Isogen Bioscience BV). The 19-mer phosphorothioate oligonucleotide AS (5′-CGCCGCTGCTGGGGCCATG-3′) is complementary to dMAL mRNA, whereas oligonucleotide AM (5′-CGCGGCCACTCGCGTCGTG-3′) is similar in composition to AS but contains some replacements to prevent pairing with dMAL mRNA. Oligonucleotides were introduced into MDCK cells by electroporation. This was carried out in the presence or absence of oligonucleotides AS or AM at 18 μM in 4-mm gap cuvettes by using Electro Cell Manipulator 600 equipment set up at 1.6 kV, 24 Ω, and 50 μF. Under these conditions the actual pulse length obtained in different experiments, as defined by the equipment manufacturer, ranged from 0.5 to 1 ms. Parallel controls to measure the efficiency of the transfection were performed by immunofluorescence analysis with phosphorothioate oligonucleotides labeled with Texas red at the 5′ end.

Detergent Extraction Procedures

GEMs were isolated by standard procedures (Brown and Rose, 1992). Cells grown to confluency in 100-mm dishes were rinsed with PBS and lysed for 20 min in 1 ml of 25 mM Tris-HCl, pH 7.5, 150 mM NaCl, 5 mM EDTA, 1% Triton X-100 at 4°C. The lysate was scraped from the dishes with a rubber policeman, the dishes rinsed with 1 ml of the same buffer at 4°C, and the lysate homogenized by passing the sample through a 22-gauge needle. The extract was finally brought to 40% sucrose in a final volume of 4 ml and placed at the bottom of an 8-ml 5–30% linear sucrose gradient. Gradients were centrifuged for 18 h at 39,000 rpm at 4°C in a Beckman SW41 rotor. 1-ml fractions were harvested from the bottom of the tube and aliquots were subjected to immunoblot analysis. The method of Skibbens et al. (1989) was adopted to analyze the partition of HA into insoluble membranes. In brief, cell monolayers were extracted for 20 min on ice with 25 mM Tris-HCl, pH 7.5, 150 mM NaCl, 5 mM EDTA, 1% Triton X-100 supplemented with a cocktail of proteases. The extracts were then centrifuged in a refrigerated Hettich microfuge at 14,000 rpm for 1 min. The supernatant (soluble fraction) was removed, and a small amount of the remaining soluble material was recovered from the pellet (insoluble fraction) after a second centrifugation. The soluble material was pooled, and the pellet resuspended in buffer for SDS-PAGE. Finally, equivalent aliquots from the soluble and insoluble fractions were subjected to SDS-PAGE and analyzed by autoradiography or immunoblotting.

Immunoblot and Immunoprecipitation Analyses

For immunoblot analysis, samples were subjected to SDS-PAGE in 15% acrylamide gels under reducing conditions and transferred to Immobilon-P membranes (Millipore). After blocking with 5% (wt/vol) nonfat dry milk, 0.05% (vol/vol) Tween 20 in PBS, blots were incubated with the indicated primary antibody. After several washings, blots were incubated for 1 h with goat anti–mouse (or anti–rat) IgG antibodies coupled to horseradish peroxidase, washed extensively, and developed using an enhanced chemiluminescence Western blotting kit (ECL; Amersham). Quantitative analyses were done with the 300A computing densitometer (Molecular Dynamics).

For metabolic labeling, cells were starved in culture medium lacking methionine and cysteine for 30 min and incubated with 100–500 μCi of a [^{35}S]methionine/cysteine mixture (ICN) for 10 min at 37°C. After this period, the medium was removed and replaced with standard culture medium. To be used in immunoprecipitation studies, antibodies were prebound overnight at 4°C to protein G–Sepharose in 10 mM Tris-HCl, pH 8.0, 0.15 M NaCl, 1% Triton X-100. Cell extracts prepared with 1% Triton X-100 at 37°C or in the presence of 60 mM octyl-glucoside were centrifuged at 14,000 rpm in a microfuge, and the supernatants were incubated for 4 h at 4°C with a control anti-CD4 mAb bound to protein G–Sepharose. After centrifugation, the supernatant was immunoprecipitated by incubation for 4 h at 4°C with mAb 9E10 bound to protein G–Sepharose. The immunoprecipitates were collected, washed six times with 1 ml of 10 mM Tris-HCl, pH 8.0, 0.15 M NaCl, 1% Triton X-100, and analyzed by SDS-PAGE under reducing conditions. Immunoprecipitation of surface-biotinylated proteins was carried out with streptavidin-agarose using a protocol similar to that described for immunoprecipitation with antibodies bound to protein G–Sepharose. To detect ^{35}S-labeling, dried gels were finally exposed to imaging plates (Fuji Photo Film Co.). Quantitative analyses were done with the 300A computing densitometer.

Domain-selective Biotinylation

For separate access to apical or basolateral domains, MDCK cells were seeded at confluent levels on 24-mm polyester tissue culture inserts of 0.4-μm pore size (Transwell; Costar, Inc.). The integrity of the cell monolayer was monitored by measuring the transepithelial electric resistance using the Millicell ERS apparatus (Millipore Corp.). For metabolic labeling of cells in filters, cells infected with influenza virus for 2.5 h were starved in media lacking methionine and cysteine. After 15 min, 250 μCi [^{35}S]methionine/cysteine was added to the basolateral compartment, and filters were incubated for 2 h at 37°C. After repeated washings with ice-cold PBS containing 0.1 mM $CaCl_2$ and 1 mM $MgCl_2$, 0.5 mg/ml sulfo-NHS-biotin were added either to the apical or basolateral compartment of the filter chamber. After 30 min at 4°C, the solution was removed and remaining unreacted biotin quenched by incubation with ice-cold serum-free DME. Cell monolayers were finally washed with PBS and extracted with 0.5 ml of 25 mM Tris-HCl, pH 7.5, 150 mM NaCl, 5 mM EDTA, 1% Triton X-100, 60 mM octyl-glucoside for 30 min on ice. Extracts were immunoprecipitated with streptavidin-agarose, and the immunoprecipitates fractionated by SDS-PAGE. To detect the presence of ^{35}S-labeled HA on the cell surface, blots were exposed to imaging plates. To detect surface E-cadherin, the streptavidin-agarose immunoprecipitates were analyzed by immunoblot with anti–E-cadherin antibodies.

Results

Generation and Characterization of a Novel Anti-dMAL mAb

We have reported previously the generation of mAb 6D9, which recognizes hMAL but is unreactive to dMAL (Martín-Belmonte et al., 1998). We have followed a strategy similar to that used for the generation of anti-hMAL antibodies to produce a novel anti-dMAL antibody. The peptide comprising amino acids 114–123 of dMAL was synthesized and coupled to keyhole limpet hemocyanin. The alignment of the selected canine decapeptide with the corresponding region of hMAL is shown in Fig. 1 A. Spleen cells from Wistar rats immunized with the canine peptide were fused with myeloma cells. During screening of hybridoma culture supernatants for anti-dMAL antibodies, a hybridoma clone (named 2E5) producing antibodies reactive with a protein of the predicted size of MAL (17 kD) was identified by immunoblot analysis of GEM fractions obtained from MDCK cells. To demonstrate that 2E5 mAb does indeed recognize dMAL, tagged forms of hMAL and dMAL were transiently expressed in COS-7 cells. Total cell lysates were prepared 24 h after transfection and subjected to immunoblot analysis with either 6D9, 2E5, or anti-tag 9E10 mAb. Fig. 1 B shows that, whereas mAb 6D9 recognizes hMAL but not dMAL as reported previously (Martín-Belmonte et al., 1998), mAb 2E5 is not reactive with hMAL but recognizes dMAL. As a control of the efficiency of the transfections, aliquots from the same samples were analyzed with anti-tag 9E10 mAb.

Endogenous MAL Is Exclusively Confined to GEMs in MDCK Cells

The GEM fraction, which is resistant to solubilization by nonionic detergent at low temperatures, can be separated from the bulk of cellular membranes, which are solubilized by the detergent, and from cytosolic proteins by using an established protocol involving centrifugation to equilibrium on sucrose density gradients (Brown and Rose, 1992). To analyze the distribution of dMAL, MDCK cells

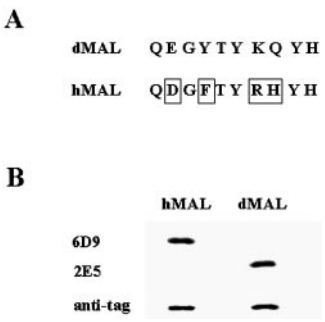

Figure 1. Characterization of a novel mAb to dMAL. (A) Sequence alignment of amino acids 114–123 of dMAL and hMAL. The indicated decapeptide corresponding to the canine sequence was used for the preparation of antibodies to the dMAL protein. The amino acid replacements of this sequence in hMAL are boxed. (B) Characterization of the anti-dMAL mAb 2E5. Protein extracts from COS-7 cells transiently expressing either hMAL or dMAL tagged with the c-Myc 9E10 epitope were subjected to immunoblot analysis with mAb 6D9, mAb 2E5, or anti-tag mAb 9E10. As COS-7 cells are negative for *MAL* gene expression (not shown), no reactivity was observed with endogenous proteins of COS-7 cells.

were extracted with 1% Triton X-100 at 4°C, and the extracts were centrifuged to equilibrium. 12 1-ml fractions were obtained after fractionation of the gradient from the bottom of the tube. When the different fractions were analyzed by immunoblotting with anti-MAL 2E5 mAb, MAL was detected exclusively as being present in the floating detergent-resistant membrane fractions, indicating that endogenous MAL specifically resides in GEMs in MDCK cells (Fig. 2). The distribution of caveolin and calnexin along the gradient, as respective representatives of proteins included (Kurzchalia et al., 1992; Sargiacomo et al., 1993) or excluded (Lee et al., 1998) from GEMs, are shown as internal controls of the fractionation procedure.

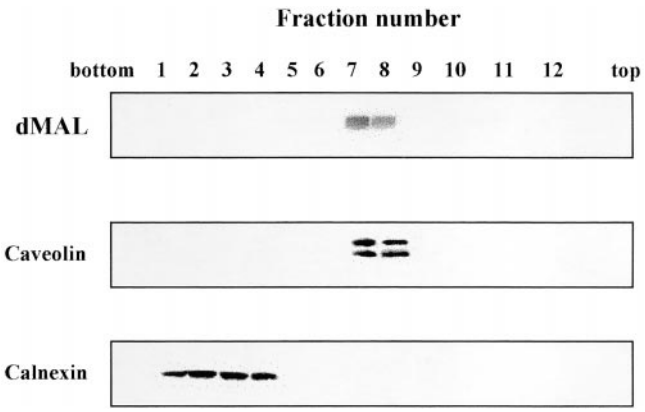

Figure 2. Identification of endogenous MAL in GEM microdomains in MDCK cells. Epithelial MDCK cells were extracted with 1% Triton X-100 at 4°C, and subjected to centrifugation to equilibrium in sucrose density gradients. 1-ml fractions were collected from the bottom of the tube. Fractions 1–4 are the 40% sucrose layer and contain cytosolic proteins and the bulk of cellular membranes, whereas fractions 5–12 are the 5–30% sucrose layer and contain GEMs. Aliquots from each fraction were subjected to SDS-PAGE and analyzed by immunoblotting with anti-MAL mAb 2E5. The distributions of caveolin, a membrane protein found in caveolar GEMs, and of calnexin, an endoplasmic reticulum transmembrane protein excluded from GEMs, were analyzed in parallel as internal controls of the fractionation procedure.

Depletion of Endogenous MAL in MDCK Cells by Using an Antisense Oligonucleotide-based Strategy

To approach directly the possible role of MAL in apical transport, we designed a 19-mer phosphorothionate oligonucleotide complementary to the sequence surrounding the AUG translation initiation site of dMAL mRNA (oligonucleotide AS) and a control oligonucleotide (oligonucleotide AM) with a composition similar to that of AS, but differing from it in seven nucleotides scattered along its sequence (Fig. 3 A). These oligonucleotides were transfected by electroporation into MDCK cells and 48 h later, MDCK cell extracts were analyzed by immunoblotting with mAb 2E5. Fig. 3 B shows that whereas the control oligonucleotide AM did not affect the levels of MAL, transfection of oligonucleotide AS greatly diminished the amount of endogenous MAL in MDCK cells. The extent of the depletion varied between experiments, probably due to differences in the actual pulse length set up by the electroporation device in each transfection. Parallel experiments using Texas red–labeled phosphorothioate oligonucleotides indicated that the efficiency of transfection varied between 80 and 99% of the cells as assayed by immunofluorescence analysis (not shown). The MAL levels obtained in cells electroporated with oligonucleotide AS were usually 10–80% of the amount of MAL found in cells electroporated with oligonucleotide AM. The levels of caveolin (Kurzchalia et al., 1992; Sargiacomo et al., 1993) and that of the amyloid precursor protein (Ikezu et al., 1998; Lee et al., 1998), two proteins found in GEMs in MDCK cells, were not affected by this treatment (Fig. 3 B). When the effect of oligonucleotide AS was assayed on MDCK cells ectopically expressing a tagged form of hMAL, we found that whereas the endogenous dMAL protein was depleted, the levels of the exogenously expressed protein were almost completely unaffected (Fig. 3 C). This is probably due to the fact that both the insertion of sequences encoding the c-Myc 9E10 epitope after the translation initiation codon, and the presence of a base change in the human sequence in the region covered by oligonucleotide AS, reduce the number of nucleotides that pair with the ectopic hMAL mRNA species (Fig. 3 A). In addition, the presence of the c-Myc epitope-encoding sequences separates oligonucleotide AS from the translation initiation site, which is generally considered to be one of the best target sites for obtaining good depletions with antisense oligonucleotides (Wagner, 1994).

MAL Affects the Levels of HA in Detergent-insoluble Membranes

Taking into account the previously proposed role of MAL in raft organization (Puertollano et al., 1997), we first investigated whether or not MAL levels affect the presence of HA in GEMs as measured by insolubility in 1% Triton X-100 at 4°C using the sedimentation procedure described by Skibbens et al. (1989). MDCK cells were transfected with oligonucleotides AM or AS, and infected 48 h later with influenza virus. After 2.5 h, cells were labeled with [^{35}S]methionine/cysteine for 10 min, and chased for 2 h in normal medium. The soluble and insoluble fractions were separated by centrifugation in a microfuge after extraction of the cells with 1% Triton X-100 at 4°C, and were sub-

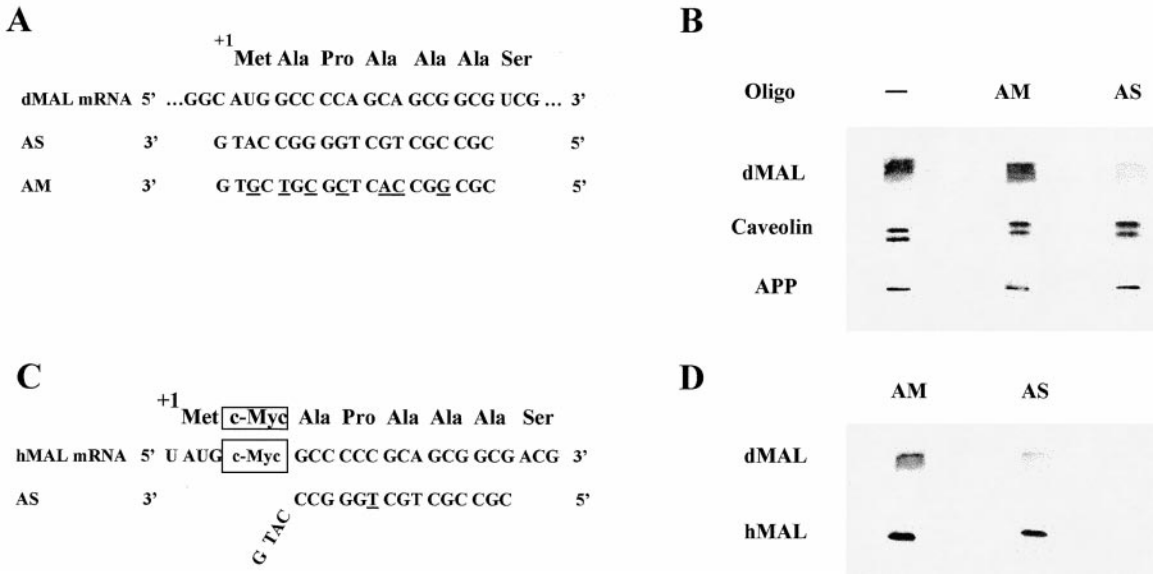

Figure 3. Depletion of endogenous MAL in MDCK cells by transfection with an antisense phosphorothioate oligonucleotide. (A) Nucleotide sequence of the oligonucleotides used. The sequence of the antisense oligonucleotide AS, used in MAL depletion experiments, and its alignment with dMAL mRNA are shown. Note that oligonucleotide AS covers the AUG translation initiation site and the triplets for the first NH_2-terminal amino acids of dMAL. Control oligonucleotide AM is similar to oligonucleotide AS MAL but contains seven substitutions (underlined) that mismatch with the dMAL mRNA sequence. (B) Transfection of oligonucleotide AS in MDCK cells causes a drop in endogenous dMAL protein levels. MDCK cells were electroporated in the presence of oligonucleotide AM or AS or in their absence, and incubated at 37°C. After 48 h, cell extracts were subjected to immunoblot analysis with anti-MAL mAb 2E5 or with antibodies to caveolin or to amyloid precursor protein (APP). (C) Alignment of oligonucleotide AS with the engineered hMAL mRNA encoding the hMAL protein tagged with the c-Myc 9E10 epitope. The presence of the sequences encoding the c-Myc epitope and of a silent base substitution (underlined) in engineered hMAL mRNA prevents perfect pairing with oligonucleotide AS. In addition, the presence of the c-Myc encoding sequences separates oligonucleotide AS from the AUG translation initiation site. (D) Engineered hMAL is resistant to depletion by oligonucleotide AS. MDCK cells stably expressing tagged hMAL were electroporated in the presence of oligonucleotide AM or AS and incubated at 37°C. After 48 h, cell extracts were subjected to immunoblot analysis with either anti-MAL 2E5 (dMAL) or anti-tag (hMAL) antibodies.

jected to SDS-PAGE and autoradiographed. Viral proteins were easily identified due to the profound shut-off of host protein synthesis induced by influenza virus infection (not shown). For simplicity, only the band corresponding to HA is shown in the experiments presented here. The extent of MAL depletion was quantified by densitometric analysis of immunoblots of the initial lysates from cells transfected with either oligonucleotide AM or AS with mAb 2E5, and the partition of radiolabeled HA into the soluble and insoluble fractions was measured by densitometric analysis of the autoradiograms. Fig. 4 B shows the partition of HA in cells with the indicated levels of endogenous MAL. Fig. 4 A shows, as an example of those experiments, the partition of HA in the soluble and insoluble fractions under conditions in which the endogenous MAL levels were ~15% of those in control cells. As shown in Fig. 4, A and B, HA insolubility decreased progressively with the reduction of MAL levels, indicating that MAL might favor HA residence within GEMs. The insolubilities of caveolin and amyloid precursor protein were not affected by MAL depletion (not shown). To further address the role of MAL in HA insolubility we carried out pulse-chase experiments to analyze the incorporation of HA into GEMs in A498 cells, which lack endogenous MAL expression (Millán et al., 1997a) and in A498/hMAL cells, which express ectopically tagged hMAL. Fig. 4, C and D, shows that although HA became progressively insoluble in normal A498 cells, the expression of MAL in these cells caused a marked increase in the insolubility of HA at all the chase times assayed. Furthermore, the effect of MAL expression in HA insolubility was not due to an artifact of the sedimentation procedure caused by differences in size of the Triton X-100–resistant membranes between A498 and A498/hMAL cells, as it also was observed when HA insolubility was assayed by floatation using centrifugation to equilibrium (Fig. 4 E).

HA Associates with MAL during Biosynthetic Transport

To examine whether there is an association between HA and MAL during transport of newly synthesized HA to the cell surface, we carried out immunoprecipitation experiments in MDCK cells infected with influenza virus. As anti-MAL 2E5 mAb works poorly in immunoprecipitation analysis, this study was performed using anti-tag mAb 9E10 and MDCK cells stably expressing tagged hMAL (MDCK/hMAL cells). Cells were infected with influenza virus, incubated at 37°C for 2.5 h, labeled for 1 h with [^{35}S]methionine/cysteine, and maintained at 20°C for 1 h to accumulate radiolabeled HA in the trans-Golgi network (Matlin and Simons, 1983). Finally, cells were extracted with 1% Triton X-100 at either 4 or 37°C, or with 1% Triton X-100 plus 60 mM octyl-glucoside. Fig. 5 A shows that,

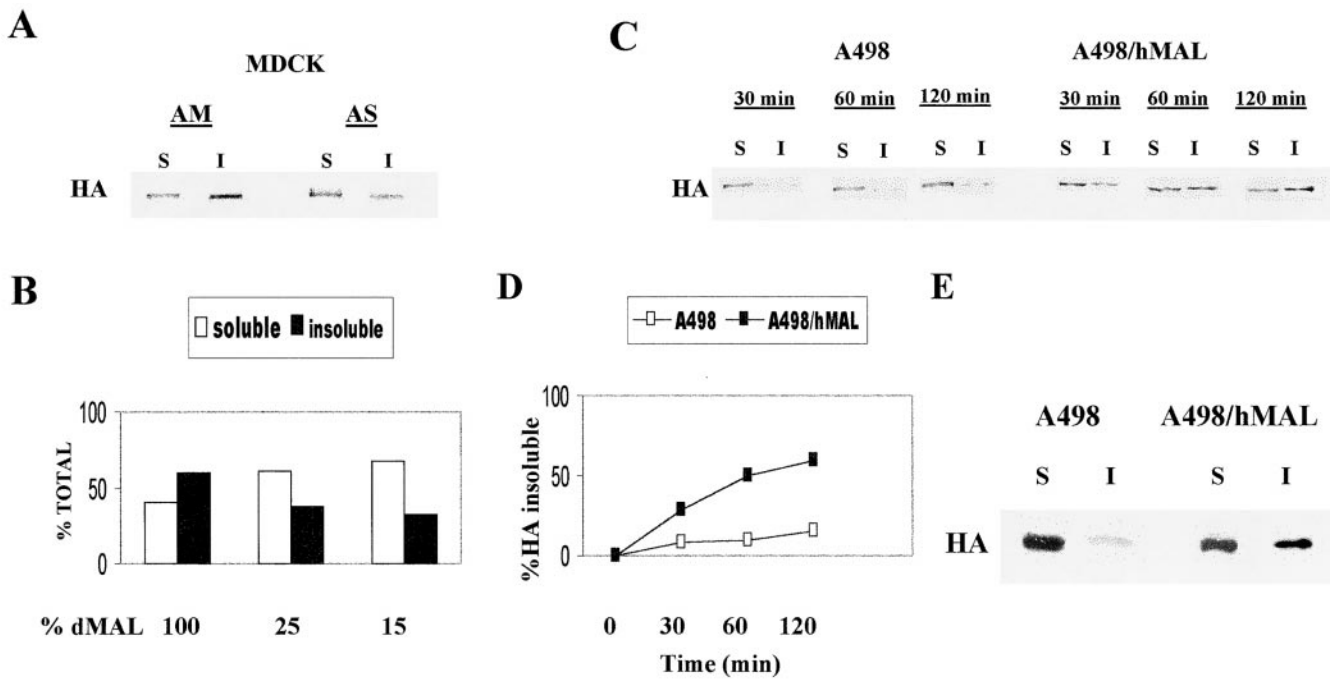

Figure 4. Effect of MAL levels on HA insolubility. (A) Effect of MAL depletion on HA insolubility in MDCK cells. MDCK cells were transfected with either oligonucleotide AM or AS, and incubated at 37°C. The amount of MAL in these cells was analyzed by immunoblotting with 2E5 mAb at 48 h after transfection to estimate the extent of MAL depletion. Simultaneously, cells were infected with influenza virus, incubated for 2.5 h, and pulse-labeled with [^{35}S]methionine/cysteine for 10 min. After a 2-h chase, cells were extracted with 1% Triton X-100 at 4°C, and the soluble (S) and insoluble (I) fractions separated by centrifugation. Finally, equivalent aliquots from these fractions were subjected to SDS-PAGE and autoradiographed. A representative experiment in which MAL levels were ~15% of those in normal cells is presented. (B) Quantitative analysis of the effect of MAL depletion on HA insolubility in MDCK cells. The HA signals present in the soluble and the insoluble fractions were quantified from experiments similar to that shown in A but in which MAL was depleted to different extents. The values are represented as percentages of radiolabeled HA in the soluble (white bars) and insoluble (black bars) fractions. The results of some representative experiments are shown. The effects observed in other experiments in which MAL was depleted to other extents, and that are not included in the figure, were in agreement with those shown. (C) Ectopic expression of MAL in MAL-deficient A498 epithelial cells enhances insolubility of HA. Normal A498 cells or A498 cells stably expressing the hMAL protein tagged with the c-Myc epitope (A498/hMAL cells) were infected with influenza virus. After 2.5 h, cells were pulse-labeled with [^{35}S]methionine/cysteine for 10 min, and chased for the indicated times. Cells were extracted with 1% Triton X-100 at 4°C, and the soluble and insoluble fractions separated by centrifugation. Aliquots from both fractions were subjected to SDS-PAGE and autoradiographed. The partition of radiolabeled HA in the soluble and insoluble fractions at the different times of chase used is shown. (D) Quantitative analysis of the incorporation of HA into the soluble and insoluble fractions in A498 and in A498/hMAL cells. The HA signals in the insoluble fractions shown in C were quantified and expressed as percentages of total radiolabeled HA. (E) Analysis by centrifugation to equilibrium of the effect of ectopic MAL expression in HA insolubility in A498 cells. A498 or A498/hMAL cells were infected with influenza virus. After 2.5 h, cells were pulse-labeled with [^{35}S]methionine/cysteine for 10 min, and chased for 30 min. Cells were then extracted with 1% Triton X-100 at 4°C, and subjected to centrifugation to equilibrium in a discontinuous sucrose density gradient. This gradient consisted of a 40% sucrose bottom layer sequentially overlaid with layers of 30% and 5% sucrose. Aliquots from the soluble (S, 40% sucrose) and insoluble (I, 5–30% interface) fractions were subjected to SDS-PAGE and autoradiographed.

in contrast with the extract prepared at 4°C, both HA and MAL are in the soluble fraction (supernatant) in the extract prepared at 37°C as assayed by the sedimentation procedure (Skibbens et al., 1989), in agreement with previous reports showing that treatment at 37°C solubilizes proteins in GEMs (Brown and Rose, 1992; Melkonian et al., 1995). To rule out the possibility that the presence of HA and MAL in the supernatant was due to differences in the size of remaining membrane complexes resistant to extraction at 37°C, the supernatant fraction was subjected to centrifugation to equilibrium in sucrose density gradients. Fig. 5 B shows that under those conditions of extraction both HA and MAL appear exclusively in the fractions containing soluble material. The supernatant from the 1% Triton X-100 extract prepared at 37°C was subsequently subjected to immunoprecipitation with anti-CD4 mAb OKT4, taken as control mAb, or with anti-tag mAb 9E10. The presence of tagged-hMAL in the immunoprecipitates was assayed by immunoblotting with mAb 9E10 and that of HA by autoradiography. The right panel of Fig. 5 C shows that HA and MAL coimmunoprecipitate in the extracts prepared at 37°C. Furthermore, this association is not the result of a redistribution of the proteins during the extraction procedure as revealed by the absence of HA in the immunoprecipitates obtained using a similar extract prepared using a mixture of ^{35}S-labeled wild-type (untransfected) MDCK cells infected with influenza virus and uninfected MDCK/hMAL cells (Fig. 5 C, middle). The

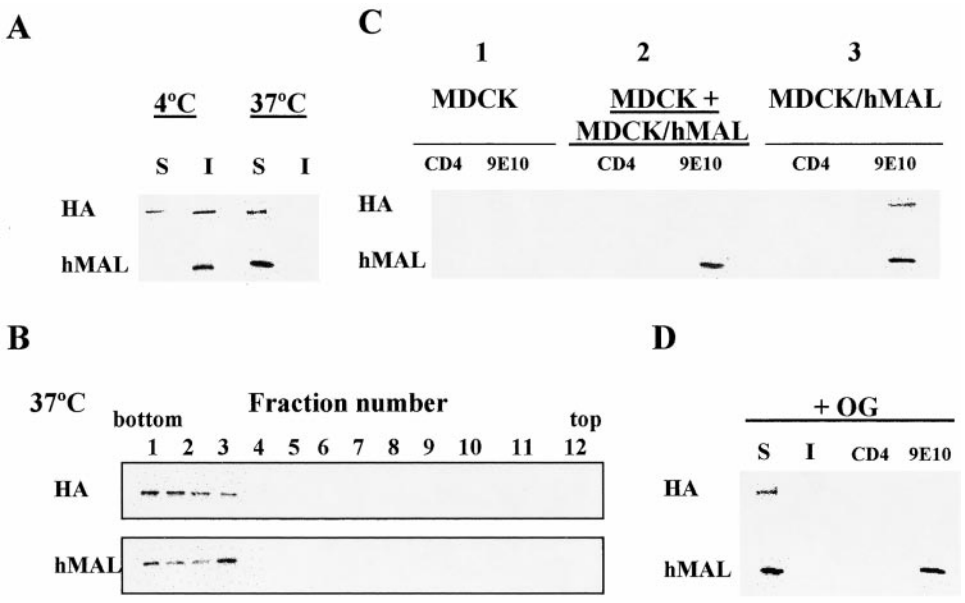

Figure 5. Association of HA with MAL during biosynthetic HA transport. (A) MDCK cells stably expressing hMAL tagged with the 9E10 c-Myc epitope (MDCK/hMAL cells) were infected with influenza virus. After 2.5 h, cells were metabolically labeled with [^{35}S]methionine/cysteine for 1 h at 37°C, and incubated for 1 h at 20°C in normal medium. Cells were extracted with 1% Triton X-100 at either 4 or 37°C, and the extracts were centrifuged. Equivalent aliquots from the supernatant (S, soluble) and from the pellet (I, insoluble) were subjected to SDS-PAGE and analyzed by autoradiography (HA) or immunoblot with mAb 9E10 (hMAL). (B) The supernatant from the extract prepared at 37°C was subjected to centrifugation to equilibrium in a sucrose density gradient. The distribution of HA was analyzed by autoradiography, and that of hMAL by immunoblotting with mAb 9E10. (C) Metabolically labeled normal MDCK cells infected with influenza virus were mixed (sample 2) or not (sample 1) with uninfected MDCK/hMAL cells. After extraction with Triton X-100 at 37°C, the extracts were centrifuged as in A and subjected to immunoprecipitation with control anti-CD4 OKT4 antibodies or with mAb 9E10 coupled to protein G–Sepharose. The immunoprecipitates were then subjected to SDS-PAGE and autoradiographed (HA) or analyzed by immunoblotting with mAb 9E10 (hMAL). A similar analysis was carried out using metabolically labeled MDCK/hMAL cells infected with influenza virus (sample 3). Coimmunoprecipitation of HA and MAL was only detected in sample 3, indicating that the observed association is not caused by redistribution of HA and MAL after detergent extraction. (D) MDCK/hMAL cells infected with influenza virus were metabolically labeled as described in A. Cells were extracted with 1% Triton X-100 + 60 mM octyl-glucoside at 37°C, and the soluble (S) and insoluble (I) fractions were separated by centrifugation. The soluble fraction was then subjected to immunoprecipitation with either anti-CD4 control antibodies or with anti-tag 9E10 mAb. The immunoprecipitates were subjected to SDS-PAGE and autoradiographed (HA) or analyzed by immunoblotting with mAb 9E10 (hMAL).

possibility of an unspecific interaction of mAb 9E10 with HA was ruled out by the absence of HA in the 9E10 mAb immunoprecipitates obtained using extracts from untransfected MDCK cells infected with influenza virus (Fig. 5 C, left). Extraction with octyl-glucoside is a second procedure widely used to solubilize proteins in GEMs (Brown and Rose, 1992; Melkonian et al., 1995). When MDCK/hMAL cells infected with influenza virus were extracted with octyl-glucoside, both HA and MAL appeared in the soluble fraction (Fig. 5 D, left). Immunoprecipitation of tagged-MAL with mAb 9E10 revealed that, under these conditions of solubilization, the association of HA with MAL is lost (Fig. 5 D, right).

MAL Affects the Rate of HA Delivery to the Cell Surface

The effect of MAL depletion on HA insolubility (Fig. 4) and the observed association of MAL with HA during HA biosynthetic transport (Fig. 5) led us to analyze whether MAL depletion affects the delivery of HA to the cell surface. MDCK cells were transfected with oligonucleotides AM or AS, and infected 48 h later with influenza virus. After 1 h at 37°C to allow virus adsorption and entry, cells were incubated for 2.5 h and then labeled with [^{35}S]methionine/cysteine for 10 min. Cells were chased for 0, 30, or 60 min in normal medium. Surface proteins were labeled with biotin at the end of each chase period, and biotinylated proteins were immunoprecipitated with streptavidin-agarose. The rate of arrival of newly synthesized radiolabeled HA at the cell surface was determined by autoradiography of the immunoprecipitates. Fig. 6, A and C, shows that although HA radiolabeling was similar in both cases (not shown), the kinetics of HA delivery to the plasma membrane was faster in cells transfected with control oligonucleotide AM than in cells in which MAL levels were depleted by transfection of oligonucleotide AS. When we compared the kinetics of surface arrival of HA in normal A498 cells and A498/hMAL cells, we observed that, consistent with the hypothesis of a role for MAL in HA transport, the ectopic expression of MAL in A498 cells enhanced the rate of delivery of HA to the cell surface (Fig. 6, B and C).

MAL Depletion Reduces HA Apical Transport and Causes Missorting of HA to the Basolateral Membrane

GEM disruption by lowering cell cholesterol produces reduction of apical transport and partial missorting of HA to the basolateral membrane (Keller and Simons, 1998). To examine whether MAL depletion causes a similar effect on HA transport, we compared the apical and basolateral delivery of HA in MDCK cells with either normal or depleted levels of MAL. To this end, cells were transfected with either oligonucleotides AM or AS, and seeded at high density (3.5–5.0 $\times$ 10^5 cells/cm^2) on filter culture

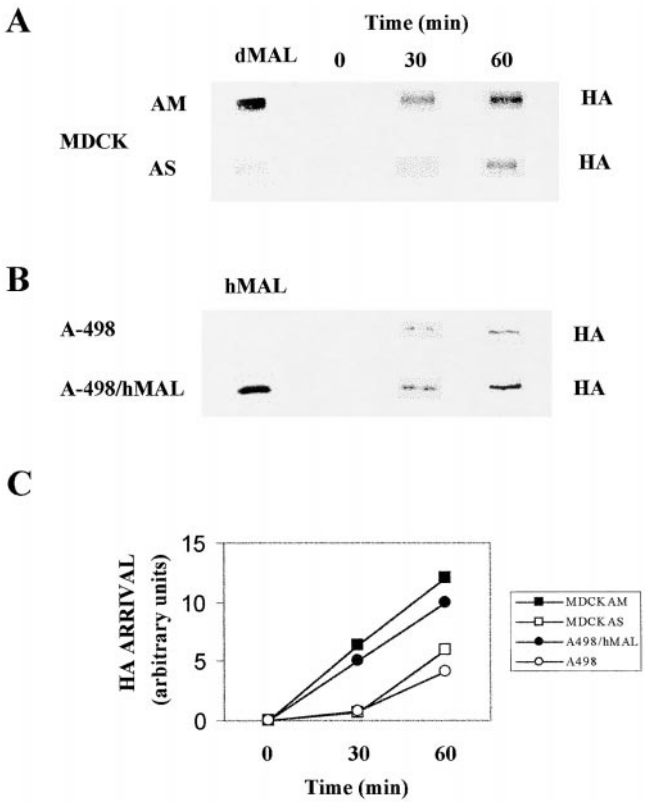

Figure 6. Effect of MAL levels on transport of HA to the cell surface. (A) Effect of MAL depletion on HA transport to the MDCK cell surface. MDCK cells were transfected with either oligonucleotide AM or AS and incubated at 37°C. The amount of MAL in these cells was analyzed by immunoblotting with 2E5 mAb at 48 h after transfection to estimate the remaining MAL levels. In the experiment shown, MAL levels were ~12% of those in control cells. These cells were infected with influenza virus, incubated for 2 h, and pulse-labeled with [^{35}S]methionine/cysteine for 10 min. Cells were then incubated at 37°C in normal medium for the indicated times. At the end of each chase period, cells were surface-labeled with sulfo-NHS-biotin at 4°C and lysed. Lysates were immunoprecipitated with streptavidin-agarose and the immunoprecipitates were subjected to SDS-PAGE. The arrival of radiolabeled HA to the cell surface was detected by autoradiography of the immunoprecipitates. The incorporation of [^{35}S]methionine/cysteine in the HA protein was similar in all cases (not shown). The results of a representative experiment are shown. The effects observed in other experiments in which MAL was depleted to other extents, and that are not included in the figure, were in agreement with those shown. (B) Ectopic expression of MAL in MAL-deficient A498 epithelial cells enhances insolubility of HA. The expression of tagged hMAL in A498/hMAL cells was monitored by immunoblotting with anti-tag 9E10 mAb. In a similar experiment to that shown in A, A498 or A498/hMAL cells were infected with influenza virus. Cells were then metabolic- and surface-labeled as described for infected MDCK cells. The autoradiogram shows the radiolabeled HA molecules that have arrived at the plasma membrane at the different times of chase assayed. (C) Quantitative analysis of the kinetics of HA arrival at the cell surface. The HA signals shown in A and B were quantified and plotted.

inserts. After 48 h at 37°C, the integrity of the cell monolayers was checked, and intact cell monolayers were infected with influenza virus. 2.5 h after removal of the inoculum, newly synthesized proteins were labeled with [^{35}S]methionine/cysteine for 2 h. Surface proteins were then separately biotinylated from the apical or basolateral face, and immunoprecipitated with streptavidin-agarose. The apical or basolateral surface expression of HA was determined by autoradiography of the corresponding streptavidin-agarose immunoprecipitate. As an internal control, the sorting of E-cadherin, a basolateral protein (Le Bivic et al., 1990), was determined by immunoblot analysis with anti–E-cadherin antibodies of the streptavidin-agarose immunoprecipitates. The extent of MAL depletion obtained in each experiment was quantified by densitometric scanning of immunoblots of the initial lysates with anti-dMAL 2E5 mAb. A representative experiment in which MAL levels dropped to ~12% of those in control cells is shown in Fig. 7 A. Whereas only 10% of surface HA was on the basolateral membrane in control MDCK cells, missorting to this domain increased to ~70% in the cells with reduced MAL levels. To confirm that the observed effects were due to MAL depletion and not to spurious effects of the AS oligonucleotide, we took advantage of the selectivity of oligonucleotide AS in blocking expression of endogenous dMAL but not of tagged hMAL in MDCK/hMAL cells to demonstrate whether ectopic expression of MAL rescues the effects observed in MAL-depleted MDCK cells. The right panel of Fig. 7 A shows that the expression of exogenous hMAL restored apical transport of HA, and prevented HA missorting to the basolateral membrane, in spite of the drop of endogenous MAL to ~12% of that in normal cells. HA insolubility was also rescued by exogenous hMAL in MDCK cells with depleted levels of the endogenous protein (not shown). A compilation of the results obtained on HA transport to the apical or basolateral membranes from experiments in which MAL was depleted to different extents is shown in Fig. 7 B. Quantitative analysis of the amount of HA on the apical or the basolateral domains indicates that the altered ratio of apical to basolateral HA targeting observed upon MAL depletion was not only due to decreased HA transport to the apical surface but also to a concomitant increased transport of HA to the basolateral surface (Fig. 7 C). Moreover, consistent with the kinetics of HA arrival at the plasma membrane in MDCK cells (Fig. 6), the total (apical + basolateral) delivery of HA to the cell surface was reduced in cells with depleted levels of MAL (Fig. 7 C). In summary, Fig. 7 indicates clear correlations between MAL depletion, progressive reduction of apical HA sorting, and concomitant increased transport of HA to the basolateral membrane.

Discussion

MAL Associates with HA and Modulates the Level of HA in GEMs

Transport of influenza virus HA to the apical membrane should be dependent on the lipid components of GEMs and the protein elements of the apical sorting machinery. Lowering the cellular cholesterol levels increases the solubility of HA in Triton X-100. This indicates that cholesterol is essential for association of HA with GEMs (Scheiffele et al., 1998). Using an antisense approach to decrease the level of MAL in MDCK cells, we have found

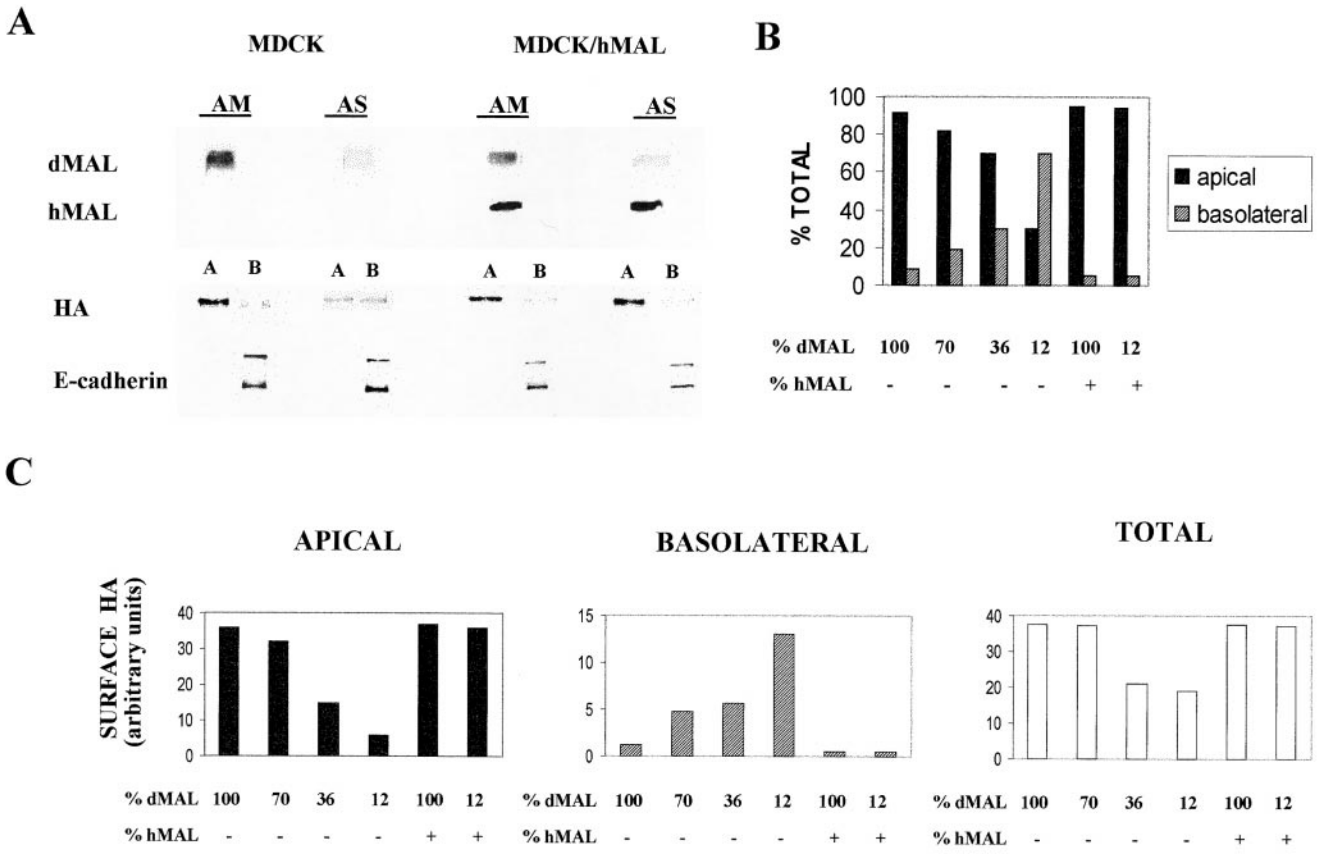

Figure 7. MAL depletion in MDCK cells causes reduced transport of HA to the apical surface and missorting to the basolateral membrane. (A) Normal MDCK cells or MDCK/hMAL cells were transfected with oligonucleotides AM or AS, and plated on 24-mm-diameter tissue culture inserts. After 48 h, cells were infected with influenza virus, and 2.5 h later were labeled with [^{35}S]methionine/cysteine for 2 h. Apical or basolateral surface proteins were then labeled in separate culture inserts with sulfo-NHS-biotin. After cell lysis, biotinylated proteins were immunoprecipitated with streptavidin-agarose. To detect apical or basolateral surface expression of HA and of E-cadherin, the immunoprecipitates were subjected to autoradiography to detect radiolabeled HA or to immunoblot analysis, respectively. The endogenous (dMAL) or the exogenous tagged hMAL levels in these cells were examined by immunoblot analysis with mAb 2E5 or 9E10, respectively. (B and C) Quantitative analysis of the effect of MAL depletion on the polarized delivery of HA. The intensities of the apical and basolateral signal corresponding to radiolabeled HA from experiments in which MAL was depleted at different extensions were quantified. The values obtained are represented as percentages of radiolabeled HA on the apical (black bars) or basolateral surface (hatched bars) (B), or expressed in arbitrary units as apical (black bars), basolateral (hatched bars), and total (apical + basolateral) surface content (white bars) of radiolabeled HA (C). The results of some representative experiments are shown. The effects observed in other experiments in which MAL was depleted to other extents, and that are not included in the figure, were in agreement with those shown.

that MAL is also required for normal incorporation of HA into GEMs. Caveolin and amyloid precursor protein, found in GEMs from caveolae or from a protein processing compartment (Kurzchalia et al., 1992; Sargiacomo et al., 1993; Ikezu et al., 1998; Lee et al., 1998), were unaffected by MAL depletion, indicating that the observed effect was specific for HA, and that MAL depletion does not affect the insolubility of proteins sequestered in other types of GEM rafts. This might be interpreted as meaning that although HA does not need MAL to gain access into GEMs, the presence of MAL favors the interaction of HA with rafts. This interpretation is supported by the following observations. In A498 cells, which lack endogenous MAL expression, the levels of HA in GEMs were lower than those in MDCK cells. Ectopic expression of MAL in A498 cells caused a dramatic increase in the levels of HA in GEMs. Thus, it is plausible that HA gains access into GEMs by itself, requiring specific residues in its transmembrane domain (Lin et al., 1998; Scheiffele et al., 1998), and that the presence of MAL helps the incorporation of HA into GEMs either through a direct interaction with HA or, indirectly, by affecting the GEM rafts.

GEM-dependent transport of influenza virus HA involves incorporation of HA into GEMs, formation of transport vesicles, and targeting and delivery of HA to the apical membrane. Based on the behavior of a panel of HA mutants, a multistep process for the initial steps of apical transport has been postulated (Lin et al., 1998). According to this model, at least some of the integral membrane components of the sorting machinery acting in the GEM-mediated pathway of apical transport are totally sequestered in GEMs. These elements would come into contact with integral proteins capable of access into GEM rafts, and only proteins able to interact with the machinery would be effi-

ciently concentrated and effectively sorted to the apical surface. Using the newly generated 2E5 mAb to dMAL protein, we have demonstrated that endogenous MAL is exclusively confined to GEM microdomains in MDCK cells. Moreover, using MDCK cells infected with influenza virus we have found that HA associates with MAL during biosynthetic transport. This association is preserved when the extracts are prepared with 1% Triton X-100 at 37°C but is lost in the presence of octyl-glucoside. The effect of octyl-glucoside indicates that either HA and MAL are not directly associated or simply that, similar to protein–lipid interactions in GEMs, their direct protein–protein interaction is sensitive to octyl-glucoside. Our results showing coimmunoprecipitation of HA and MAL in Triton X-100 extracts prepared at 37°C indicate that if there are still any lipids maintaining the association between these two proteins, those lipids are not sufficient to provide buoyancy to the HA–MAL complex as assayed by centrifugation to equilibrium or to make the complex sedimentable under conditions used to sediment GEMs.

MAL Affects the Rate of HA Transport to the Cell Surface

The decrease in the insolubility of HA in MAL-depleted MDCK cells correlated with a partial inhibition on HA transport to the plasma membrane. This is consistent with recent findings showing that the rate of arrival of HA at the plasma membrane was diminished in cells in which HA insolubility was lowered by removal of cholesterol (Keller and Simons, 1998). This indicates that both cholesterol and MAL are required for normal transport of HA to the cell surface. As evidence for the role of MAL in HA transport, we have found that the enhanced incorporation of HA in GEMs by ectopic expression of hMAL in A498 cells is accompanied by an increase in the rate of transport of HA to the cell surface. As HA is delivered to the plasma membrane in cells that lack MAL expression (e.g., wild-type A498 cells), it is obvious that MAL is not strictly necessary for transport of HA to the cell surface. Rather, we speculate that MAL is only necessary for a specialized route of transport involving GEMs that takes place only in a restricted range of cell types.

MAL Is Required for Sorting of HA to the Apical Surface in MDCK Cells

The proposed roles of MAL GEM-mediated transport led us to examine the obvious possibility that MAL is an element of the apical transport machinery in MDCK cells. As predicted, MDCK cells with reduced MAL levels showed a lower HA transport to the apical surface compared with that in control MDCK cells. The loss of apical HA transport was partially compensated for by the appearance of HA at the basolateral surface. These results resemble those obtained in MDCK cells with GEM rafts disrupted by cholesterol depletion (Keller and Simons, 1998) or with HA mutants unable to access GEMs (Lin et al., 1998) in which HA was also partially missorted to the basolateral membrane. Thus, although HA is normally excluded from basolateral vesicles, it appears that the lack of stabilization of HA into GEMs produced by MAL removal induced partial incorporation of HA into vesicles destined for the basolateral surface. The fact that ectopic expression of hMAL prevented the effect of MAL depletion on HA insolubility and sorting strongly argues against an artifactual effect of oligonucleotide AS in HA transport.

MAL as a Component of the Integral Membrane Protein Machinery for Apical Transport

GEMs have been isolated from a variety of tissues, and their existence seems to represent a general feature influencing the function of cellular membranes (Simons and Ikonen, 1997). The MAL protein has been identified as a component of GEMs in all of the cell types in which it is expressed (Kim et al., 1995; Zacchetti et al., 1995; Martín-Belmonte et al., 1998; Millán and Alonso, 1998). The fact that *MAL* gene expression is tissue- and differentiation-specific (Alonso and Weissman, 1987; Millán and Alonso, 1998) suggests that the role of MAL in GEMs is required in only a few cell types, and that this role is probably related to a specialized function common to this restricted range of cells.

In polarized epithelial cells, endogenous MAL is localized to the apical zone, consistent with its proposed role in apical transport (Martín-Belmonte et al., 1998). Based on the extensive vesiculation induced by ectopic expression of MAL in Sf21 insect cells, MAL was proposed as being an element of the apical machinery responsible for GEM vesiculation (Puertollano et al., 1997). The vesicles induced by MAL expression in insect cells were clearly different from the caveolae-like vesicles induced by caveolin as shown by coexpression of the two proteins. Thus, it was proposed that both caveolin and MAL may belong to the vesicular transport machinery specific for GEMs but acting in the assembly of different classes of GEM microdomains (Millán et al., 1997a; Puertollano et al., 1997). Caveolin appears to be related to caveolae formation (Rothberg et al., 1992; Fra et al., 1995, Li et al., 1996), whereas our present results support the hypothesis of the involvement of MAL in apical transport.

The GEM-based model for sorting of apical proteins predicts the existence of sorting receptors responsible for recruiting cargo proteins (Simons and Wandinger-Ness, 1990). The results presented in this study show that: HA associates with MAL in GEMs during biosynthetic transport; the presence of MAL favors the incorporation of HA into GEMs; and MAL is necessary for normal apical transport and accurate sorting of HA. Thus, in addition to the proposed roles of MAL in formation of vesicles for GEM-dependent transport (Puertollano et al., 1997) and GEM trafficking (Puertollano and Alonso, 1998), MAL also plays a role in the confinement of influenza virus HA into GEMs and in its transport to the apical surface.

R. Puertollano and F. Martín-Belmonte are recipients of predoctoral fellowships from the Comunidad de Madrid. J. Millán and M. de Marco are supported by predoctoral fellowships from the Ministerio de Educación y Cultura. This work was supported by grants from the Dirección General de Enseñanza Superior (PM96-0004) and the Comunidad de Madrid (08.3/0020/1998). The Department of Immunology and Oncology is funded and supported by the Consejo Superior de Investigaciones Científicas and Pharmacia & Upjohn. An institutional grant from the Fundación Ramón Areces to Centro de Biología Molecular "Severo Ochoa" is also acknowledged.

Received for publication 18 December 1998 and in revised form 19 February 1999.

References

Alonso, M.A., and S.M. Weissman. 1987. cDNA cloning and sequence of MAL, a hydrophobic protein associated with human T-cell differentiation. *Proc. Natl. Acad. Sci. USA*. 84:1997–2001.

Alonso, M.A., L. Fan, and B. Alarcón. 1997. Multiple sorting signals determine apical localization of a nonglycosylated integral membrane protein. *J. Biol. Chem*. 272:30748–30752.

Brown, D.A., and J.K. Rose. 1992. Sorting of GPI-anchored proteins to glycolipid-enriched membrane subdomains during transport to the apical cell surface. *Cell*. 68:533–544.

Drubin, D.G., and W.J. Nelson. 1996. Origins of cell polarity. *Cell*. 84:335–344.

Eaton, S., and K. Simons. 1995. Apical, basal, and lateral cues for epithelial polarization. *Cell*. 82:5–8.

Evan, G.I., G.K. Lewis, G. Ramsay, and J.M. Bishop. 1985. Isolation of mAbs specific for human c-*myc* proto-oncogene product. *Mol. Cell. Biol.* 5:3610–3616.

Fra, A.M., E. Williamson, K. Simons, and R.G. Parton. 1995. *De novo* formation of caveolae in lymphocytes by expression of VIP21-caveolin. *Proc. Natl. Acad. Sci. USA*. 92:8655–8659.

Gausepohl, H., C. Boulin, M. Kraft, and R.W. Frank. 1992. Automated multiple peptide synthesis. *Peptide Res.* 5:315–320.

Green, R.F., H.K. Meiss, and E. Rodriguez-Boulan. 1981. Glycosylation does not determine segregation of viral envelope proteins in the plasma membrane of epithelial cells. *J. Cell Biol.* 89:230–239.

Gut, A., F. Kappeler, N. Hyka, M.S. Balda, H.-P. Hauri, and K. Matter. 1998. Carbohydrate-mediated Golgi to cell surface transport and apical targeting of membrane proteins. *EMBO (Eur. Mol. Biol. Organ.) J.* 17:1919–1929.

Hanada, K., M. Nishijima, Y. Akamatsu, and R.E. Pagano. 1995. Both sphingolipids and cholesterol participate in the detergent-insolubility of alkaline phosphatase, a glycosylphosphatidylinositol-anchored protein, in mammalian membranes. *J. Biol. Chem*. 270:6254–6260.

Harlow, E., and D. Lane. 1988. Antibodies: A Laboratory Manual. Cold Spring Harbor Laboratory, Cold Spring Harbor, NY.

Ikezu, T., B.D. Trapp, K.S. Song, A. Schlegel, M.P. Lisanti, and T. Okamoto. 1998. Caveolae, plasma membrane microdomains for α-secretase-mediated processing of the amyloid precursor protein. *J. Biol. Chem*. 273:10485–10495.

Keller, P., and K. Simons. 1997. Post-Golgi biosynthetic trafficking. *J. Cell Sci.* 110:3001–3009.

Keller, P., and K. Simons. 1998. Cholesterol is required for surface transport of influenza virus hemagglutinin. *J. Cell Biol.* 140:1357–1367.

Kim, T., K. Fiedler, D.L. Madison, W.H. Krueger, and S.E. Pfeiffer. 1995. Cloning and characterization of MVP17: a developmentally regulated myelin protein in oligodendrocytes. *J. Neurosci. Res.* 42:413–422.

Kurzchalia, T.V., P. Dupree, R.G. Parton, R. Kellner, H. Virta, M. Lehnert, and K. Simons. 1992. VIP21, a 21-kD protein is an integral component of *trans*-Golgi-network–derived transport vesicles. *J. Cell Biol.* 118:1003–1014.

Le Bivic, A., Y. Sambuy, K. Mostov, and E. Rodriguez-Boulan. 1990. Vectorial targeting of an endogenous apical membrane sialoglycoprotein and uvomorulin in MDCK cells. *J. Cell Biol.* 110:1533–1539.

Lee, S.-J., U. Liyanage, P.E. Bickel, W. Xia, P.T. Lansbury, Jr., and K.S. Kosik. 1998. A detergent-insoluble membrane compartment contains Aβ *in vivo*. *Nat. Med*. 4:730–734.

Li, S., K.S. Song, S.S. Koh, A. Kikuchi, and M.P. Lisanti. 1996. Baculovirus-based expression of mammalian caveolin in Sf21 insect cells. *J. Biol. Chem*. 271:28647–28654.

Lin, S., H.Y. Naim, A.C. Rodriguez, and M.G. Roth. 1998. Mutations in the middle of the transmembrane domain reverse the polarity of transport of the influenza virus hemagglutinin in MDCK epithelial cells. *J. Cell Biol.* 142:51–57.

Martín-Belmonte, F., L. Kremer, J.P. Albar, M. Marazuela, and M.A. Alonso. 1998. Expression of the MAL gene in the thyroid: the MAL proteolipid, a component of glycolipid-enriched membranes, is apically distributed in thyroid follicles. *Endocrinology*. 139:2077–2084.

Matlin, K.S., and K. Simons. 1983. Reduced temperature prevents transfer of a membrane glycoprotein to the cell surface but does not prevent terminal glycosylation. *Cell*. 34:233–243.

Matter, K., and I. Mellman. 1994. Mechanisms of cell polarity: sorting and transport in epithelial cells. *Curr. Opin. Cell Biol.* 6:545–554.

Melkonian, K.A., T. Chu, L.B. Tortorella, and D.A. Brown. 1995. Characterization of proteins in detergent-resistant membrane complexes from Madin-Darby canine kidney epithelial cells. *Biochemistry*. 34:16161–16170.

Millán, J., and M.A. Alonso. 1998. MAL, a novel integral membrane protein of human T lymphocytes, associates with glycosylphosphatidylinositol-anchored proteins and Src-like tyrosine kinases. *Eur. J. Immunol.* 28:3675–3684.

Millán, J., R. Puertollano, L. Fan, and M.A. Alonso. 1997a. Caveolin and MAL, two protein components of internal detergent-insoluble membranes, are in distinct lipid microenvironments in MDCK cells. *Biochem. Biophys. Res. Commun.* 233:707–712.

Millán, J., R. Puertollano, L. Fan, C. Rancaño, and M.A. Alonso. 1997b. The MAL proteolipid is a component of the detergent-insoluble membrane subdomains of human T-lymphocytes. *Biochem. J.* 321:247–252.

Puertollano, R., and M.A. Alonso. 1998. A short peptide motif at the carboxyl terminus is required for incorporation of the integral membrane MAL protein to glycolipid-enriched membranes. *J. Biol. Chem*. 233:12740–12745.

Puertollano, R., S. Li, M.P. Lisanti, and M.A. Alonso. 1997. Recombinant expression of the MAL proteolipid, a component of glycolipid-enriched membrane microdomains, induces the formation of vesicular structures in insect cells. *J. Biol. Chem*. 272:18311–18315.

Rodriguez-Boulan, E., and M. Pendergast. 1980. Polarized distribution of viral envelope glycoproteins in the plasma membrane of infected epithelial cells. *Cell*. 20:45–54.

Rodriguez-Boulan, E., and S.K. Powell. 1992. Polarity of epithelial and neuronal cells. *Annu. Rev. Cell Biol.* 8:395–427.

Rodriguez-Boulan, E.J., and D.D. Sabatini. 1978. Asymmetric budding of viruses in epithelial monolayers: a model for the study of epithelial polarity. *Proc. Natl. Acad. Sci. USA*. 75:5071–5075.

Roth, M.G., J.P. Fitzpatrick, and R.W. Compans. 1979. Polarity of influenza and vesicular stomatitis virus maturation in MDCK cells: lack of a requirement for glycosylation of viral glycoproteins. *Proc. Natl. Acad. Sci. USA*. 76: 6430–6434.

Rothberg, K.G., J.E. Heuser, W.C. Donzell, Y. Ying, J.R. Glenney, and R.G.W. Anderson. 1992. Caveolin, a protein component of caveolae membrane coats. *Cell*. 68:673–682.

Sargiacomo, M., M. Sudol, Z.-L. Tang, and M.P. Lisanti. 1993. Signal transducing molecules and glycosyl-phosphatidylinositol-linked proteins form a caveolin-rich insoluble complex in MDCK cells. *J. Cell Biol.* 122:789–807.

Schaeren-Wiemers, N., D.M. Valenzuela, M. Frank, and M.E. Schwab. 1995. Characterization of a rat gene, rMAL, encoding a protein with four hydrophobic domains in central and peripheral myelin. *J. Neurosci.* 15:247–252.

Scheiffele, P., M.G. Roth, and K. Simons. 1998. Interaction of influenza virus haemagglutinin with sphingolipid-cholesterol membrane domains via its transmembrane domain. *EMBO (Eur. Mol. Biol. Organ.) J.* 16:5501–5508.

Simons, K., and E. Ikonen. 1997. Functional rafts in cell membranes. *Nature*. 387:569–572.

Simons, K., and G. van Meer. 1988. Lipid sorting in epithelial cells. *Biochemistry*. 27:6197–6202.

Simons, K., and A. Wandinger-Ness. 1990. Polarized sorting in epithelia. *Cell*. 62:207–210.

Skibbens, J.E., M.G. Roth, and K.S. Matlin. 1989. Differential extractability of influenza virus hemagglutinin during intracellular transport in polarized epithelial cells and nonpolar fibroblasts. *J. Cell Biol.* 108:821–832.

Thomas, D.C., and M.G. Roth. 1994. The basolateral targeting signal in the cytoplasmic domain of glycoprotein G from vesicular stomatitis virus resembles a variety of intracellular targeting motifs related by primary sequence but having diverse targeting activities. *J. Biol. Chem*. 269:15732–15739.

Traub, L.M., and S. Kornfeld. 1997. The *trans*-Golgi network: a late secretory station. *Curr. Opin. Cell Biol.* 9:527–533.

Wagner, R.W. 1994. Gene inhibition using antisense oligodeoxynucleotides. *Nature*. 372:333–335.

Zacchetti, D., J. Peranen, M. Murata, K. Fiedler, and K. Simons. 1995. VIP17/MAL, a proteolipid in apical transport vesicles. *FEBS Lett.* 377:465–469.